SAND74-0379
Unlimited Release

An Investigation of Rotation-Induced Stresses of Straight and of Curved Vertical-Axis Wind Turbine Blades

When printing a copy of any digitized SAND Report, you are required to update the markings to current standards.

L. V. Feltz, B. F. Blackwell

Prepared by Sandia Laboratories, Albuquerque, New Mexico 87115 and Livermore, California 94550 for the United States Energy Research and Development Administration under Contract AT(29-1)-789

Printed March 1975

Sandia Laboratories
energy report

SF 2900-QQB(3-74)

Issued by Sandia Laboratories, operated for the United States Atomic Energy Commission by Sandia Corporation.

NOTICE

This report was prepared as an account of work sponsored by the United States Government. Neither the United States nor the United States Atomic Energy Commission, nor any of their employees, nor any of their contractors, subcontractors, or their employees, makes any warranty, express or implied, or assumes any legal liability or responsibility for the accuracy, completeness or usefulness of any information, apparatus, product or process disclosed, or represents that its use would not infringe privately owned rights.

SF 1004-DF(2-74)

SAND74-0379
Unlimited Release
Printed March 1975

AN INVESTIGATION OF ROTATION-INDUCED STRESSES OF STRAIGHT AND OF CURVED VERTICAL-AXIS WIND TURBINE BLADES

L. V. Feltz
B. F. Blackwell
Aerodynamics Projects Department, 5620
Sandia Laboratories
Albuquerque, NM 87115

ABSTRACT

The feasibility of using straight blades for a Darrieus-type vertical-axis wind turbine is explored. Rotationally induced stresses for both straight and curved blades are compared. The scale-up implications are considered. The straight-bladed configuration does not appear to be practical because of the bending stresses induced by centrifugal forces.

CONTENTS

	Page
Introduction	7
Blade Design Considerations	8
Straight-Blade Stress Calculations	10
Addition of Restraining Straps	12
Reduction of Maximum Turbine Rotational Speed	13
Increase of Chord Thickness	14
Troposkien Blade Stress Calculations	14
Scale-Up Potential	15
Conclusions	15
Appendix A - Development of Scale-Up Stress Predictions	17
References	19

ILLUSTRATIONS

Figure		Page
1	Vertical-Axis Wind Turbine (curved blades)	8
2	Squirrel-Cage Configuration (straight blades)	8
3a	NACA 0012 Airfoil	9
3b	NACA 0024 Airfoil	9
4	Darrieus Turbine Performance	10
5a	Blade Loading Problem Definition	11
5b	Blade Equivalent Load	11
6a	Spacing of Radial Restraining Straps	13
6b	Equivalent Beam Loading	13

LIST OF SYMBOLS

a	Centrifugal acceleration
A	Cross-sectional area of blade material
c	Maximum airfoil half thickness
d	Spacing between intermediate blade supports
D	Wind turbine diameter
E	Young's modulus
F_L	Total centrifugal blade load
g	Gravitational acceleration (32.2 ft/s^2)
H	Wind turbine blade height
I	Area moment of inertia
ℓ	Beam length
M	Bending moment
r	Wind turbine radius
S	Blade stress
t	Blade skin thickness
T	Blade tensile load
V	Windspeed
V_B	Blade instantaneous linear velocity
y	Perpendicular distance from area moment-of-inertia axis
w	Blade linear load distribution
W	Total blade weight
α	Rotational acceleration
σ	Tensile yield strength
ρ	Blade material density
ω	Turbine rotational velocity
$\propto$	Proportionality symbol

AN INVESTIGATION OF ROTATION-INDUCED STRESSES OF STRAIGHT AND OF CURVED VERTICAL-AXIS WIND TURBINE BLADES

Introduction

In 1925, G. J. M. Darrieus, Paris, France, proposed for United States patent a new type of wind turbine designed for the generation of power. The patent, issued in 1931 as Number 1,835,018, was for a "turbine having its rotating shaft transverse to the flow of the current." A similar wind turbine was independently developed by the National Aeronautical Establishment of the National Research Council of Canada in the late 1960's. An artist's conception of this type of wind turbine is shown in Figure 1. The Darrieus patent statement indicates that each blade should "have a stream-line outline curved in the form of a skipping rope." A mathematical equation presented by Blackwell and Reis[1, 2] describes this "skipping rope" shape, which was given the name troposkien (from the Greek: τροπος, turning, and σνοlνlον, rope). This study also disclosed that the troposkien shape is not affected by a variation of the rotational velocity. If the blades are curved in the troposkien shape during fabrication, rotation will not cause the blades to deform as a result of bending loads; therefore, the stresses will be pure tension.

When the operation of the Darrieus-type vertical-axis wind turbine is explained to a person unfamiliar with the magnitude of centrifugal stresses that can be developed in large rotating machinery, the initial reaction invariably is "Why not use straight blades instead of curved blades?" This straight-bladed configuration, given the name squirrel cage,* is shown in Figure 2. The reasons usually quoted for preferring the squirrel-cage configuration are (1) increased aerodynamic efficiency because more of the blade is vertical and (2) increased swept area and hence increased power production. Both of these reasons are valid; nevertheless, the design considerations of a practical squirrel-cage wind turbine must also include the centrifugal forces acting on the straight blades.

The purpose of this report is to demonstrate that, because of large centrifugally induced bending stresses, the squirrel-cage rotor concept is not feasible.

---

*This configuration was also covered in the original Darrieus patent.

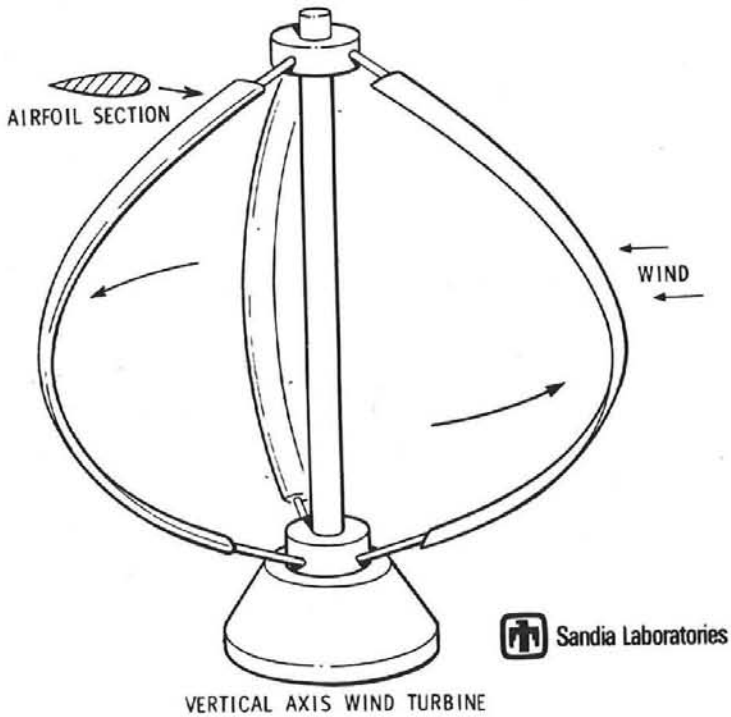

Figure 1. Vertical-Axis Wind Turbine (curved blades)

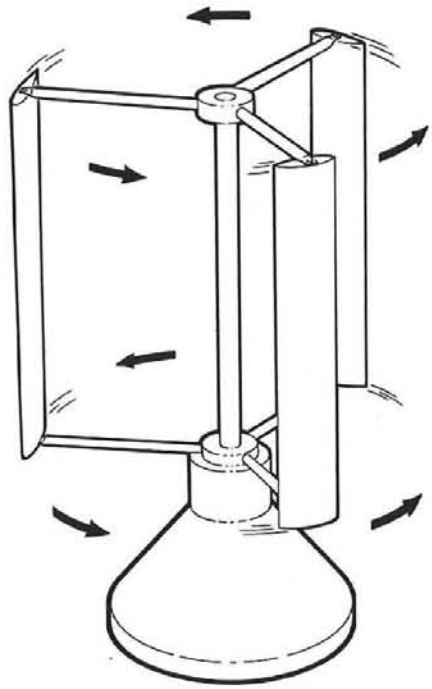

Figure 2. Squirrel-Cage Configuration (straight blades)

Blade Design Considerations

Sandia Laboratories has had a 15-foot-diameter vertical-axis wind turbine test bed of the Darrieus type in operation since May 1974. The blades are curved in an approximate troposkien shape. Curved blades and those of a squirrel-cage configuration of similar height and with a diameter of 15 feet are analyzed, and the rotationally induced stresses of the two configurations compared.

The aerodynamic cross section of the 15-foot (4.57-m)-diameter test bed blades is the symmetrical NACA 0012* profile (Figure 3a). The airfoil chord used for these analyses is 6 inches (15.24 cm) and has a maximum thickness of 0.72 inch (1.83 cm).

*The maximum thickness is 12 percent of the chord.

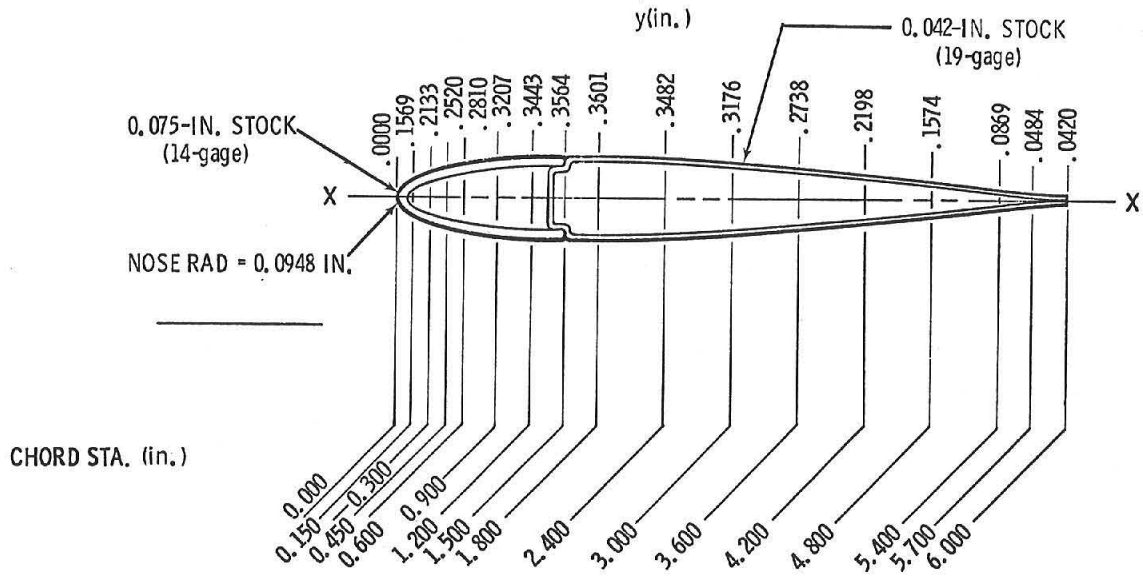

Figure 3a. NACA 0012 Airfoil

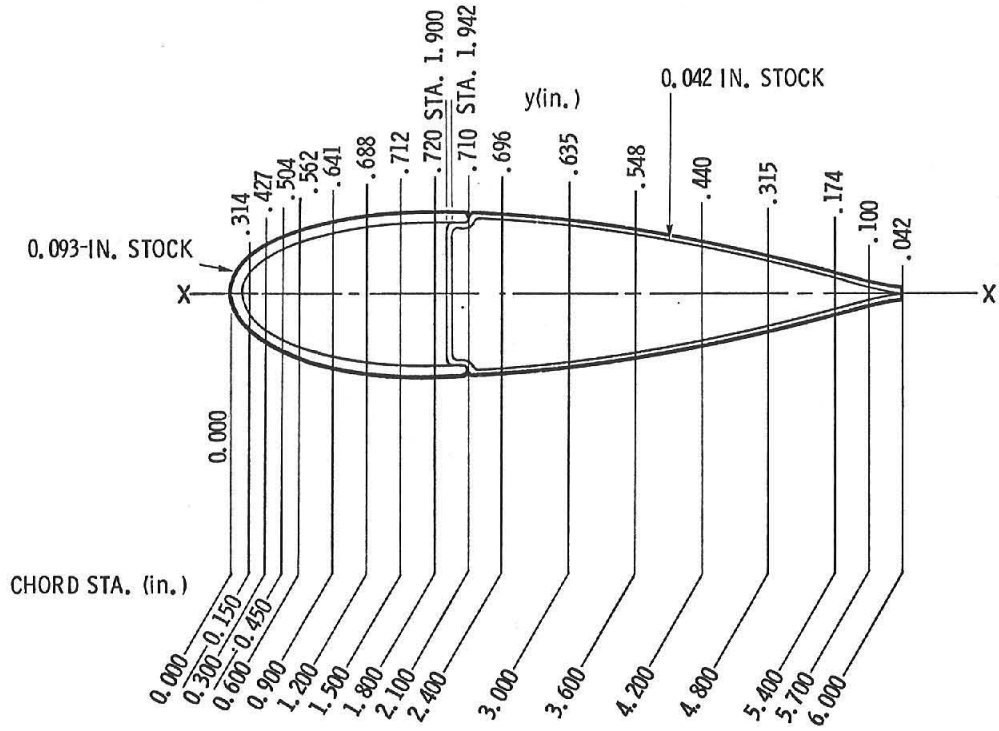

Figure 3b. NACA 0024 Airfoil

Figure 3a represents a blade that could be easily manufactured as a straight section with roll-forming or break-press techniques. The moments and cross-sectional area were determined through use of the Sandia AREA.BAS numerical computer program:

$$I_{xx} = 0.038 \text{ in.}^4 \ (1.58 \text{ cm}^4)$$
$$A = 0.642 \text{ in.}^2 \ (4.14 \text{ cm}^2). \qquad (1)$$

Next, it was considered that the material selected for such a blade should have low weight to keep the centrifugal loads down and a high modulus of elasticity to resist bending of the blade from its vertical configuration. A parameter called specific stiffness includes both of these: Specific stiffness $= \frac{E}{\rho}$ (in.) with E = modulus of elasticity (psi) and ρ = density $\left(\frac{\text{lbm}}{\text{in.}^3}\right)$.

Candidate materials included steel, aluminum, magnesium, and fiberglass. The latter two were dropped because of cost considerations and of low specific stiffness, respectively. Aluminum and steel have nearly identical specific stiffness of about 1.05×10^8 in. (2.67×10^8 cm). Another material property consideration is specific strength, which is a measure of strength versus density: Specific strength $= \frac{\sigma}{\rho}$ (in.) and σ = tensile yield strength (psi). Depending upon the particular alloy of steel or aluminum selected, the values of this parameter are comparable between 50×10^5 inches (1.3×10^6 cm) for a low-strength alloy to 80×10^5 inches (2.0×10^6 cm) for a high-strength alloy of either material. Generally the cost of steel or aluminum alloys rises as the strength of that material rises. Thus, economy dictates the selection of a steel blade for a squirrel-cage configuration because of the lower material and fabrication costs for steel.

Straight-Blade Stress Calculations

Assume that the airfoil speed is 7 times the free wind speed.[3] This would represent a turbine run-away or no-load condition as shown in Figure 4. Assume also that the free windspeed is 75 ft/s (22.9 m/s) or about 50 mph (80.5 km/hr.). This is considered to be a reasonable design goal. Figure 5a illustrates the problem to be solved.

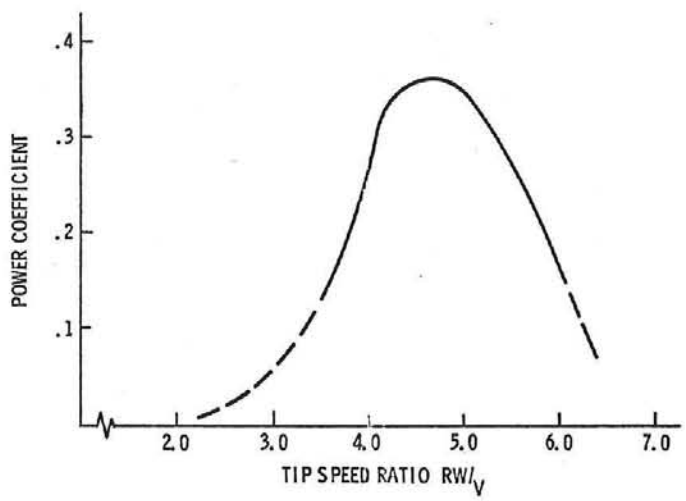

Figure 4. Darrieus Turbine Performance

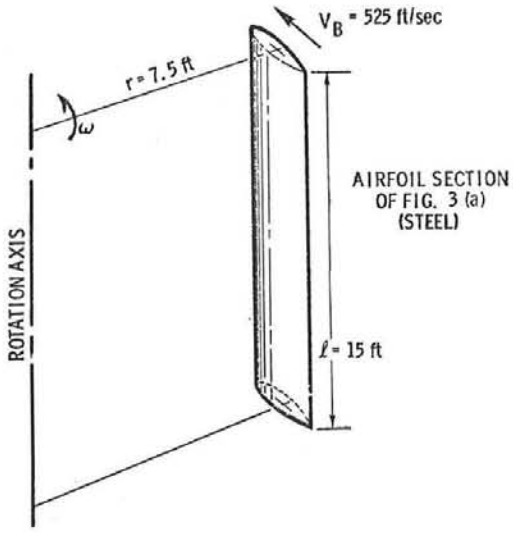

Figure 5a. Blade Loading Problem Definition

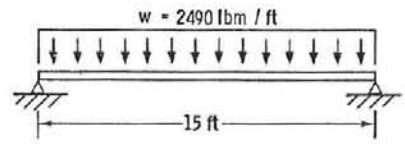

Figure 5b. Blade Equivalent Load

The blade loads can be represented as a beam loading, with uniform distribution as shown in Figure 5b.

$$\text{Blade weight} = W = A \times \ell \times 0.283 \text{ lbm/in.}^3$$

$$= 32.7 \text{ lbm } (14.8 \text{ kg}) \tag{2}$$

$$\text{Centrifugal acceleration} = \alpha = \frac{V_B^2}{r} \quad (\text{with } V_B = 7 \times 75 \text{ ft/s})$$

$$= 36,750 \text{ ft/s}^2 \ (11,200 \text{ m/s}^2)$$

or 1141 g's where

$$g = 32.2 \text{ ft/s}^2 \ (9.81 \text{ m/s}^2) \tag{3}$$

$$\text{Total blade force} = F_L = W \times g\text{'s}$$

$$= 37,300 \text{ lbf } (1.66 \times 10^5 \text{ N}) \tag{4}$$

$$\text{Load distribution} = w = F_L/\ell$$

$$= 2490 \text{ lbf/ft } (36,340 \text{ N/m}) \tag{5}$$

$$\text{Maximum moment} = M_{max} = \frac{w\ell^2}{8} = \frac{F_L \ell}{8}$$

$$= 70,000 \text{ ft-lbf } (95,000 \text{ Nm}) \tag{6}$$

$$\text{Bending stress} = \frac{M_{max}c}{I}$$

$$= 8.0 \times 10^6 \text{ psi } (5.5 \times 10^{10} \text{ N/m}^2). \tag{7}$$

Note that the calculated bending stress is much greater than the yield stress of approximately 70,000 psi (4.8×10^8 N/m^2) allowed for a typical alloy steel. Before rejecting the straight-blade concept outright, consider the allowed stress limit and accommodate it by

1. Adding intermediate restraining straps from the blade to the vertical (rotation) axis.
2. Reducing the allowed rotational velocity; i.e., prescribing milder wind operating conditions.
3. Increasing the chord thickness.

Addition of Restraining Straps

If equally spaced restraining straps are used along the blade as shown in Figure 6a, the loading between any pair of straps is equivalent to that shown in Figure 6b. For this loading the maximum moment is at the end point; i.e., under the strap attachment point to the blade:

$$M = \frac{wd^2}{12} \tag{8}$$

Combining Eqs. (7) and (8) and solving for d $\left(d = \sqrt{\frac{12\ IS}{wc}}\right)$

where

S = 70,000 psi (tensile yield stress)

I = 0.038 in.^{4}

w = 2490 lbf/ft; (F_L/ℓ)

c = 0.36 in. (chord half thickness),

yields d = 20.7 inches (0.52 m).

That is, at the velocity assumed, this airfoil would have to be radially restrained (as shown in Figure 6a) every 20.7 inches to keep the allowed bending stresses down to 70,000 psi (4.8×10^8 N/m^2). This many straps from the blade to the rotation hub (e.g., 10 per blade for 15-foot length considered) is impractical because of aerodynamic drag and also because of manufacturing cost considerations.

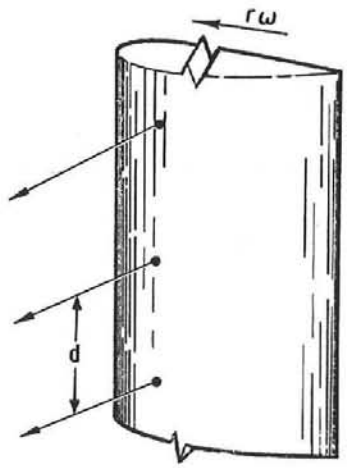

Figure 6a. Spacing of Radial Restraining Straps

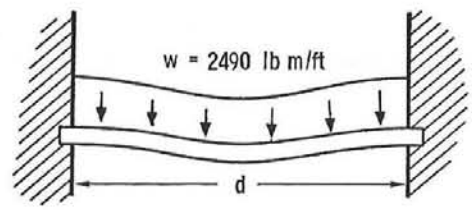

Figure 6b. Equivalent Beam Loading

Reduction of Maximum Turbine Rotational Speed

This approach will reduce the apparent load per foot (w) along the blade. Combining Eqs. (6) and (7) and solving for w yields

$$w_{max} = \frac{8\ IS}{\ell^2 c}$$

$$= 21.9 \text{ lbf/ft } (319 \text{ N/m}) \tag{10}$$

$$\frac{w_{max}}{w^*} = \frac{21.9}{2490} = 0.0088$$

(w^* from Eq. 5)

The reduced centrifugal acceleration is the product of this ratio and the results of Eq. (3).

a (reduced) = 323 ft/s^2 (98 m/s^2), or only 10 g's

From Eq. (3) the reduced blade velocity is

V_B = 49 ft/s (15 m/s).

If, as assumed, the blade speed is 7 times the windspeed, it is implied that an unsupported blade could accommodate only a 7-ft/s (2-m/s) wind. This is totally impractical from a power conversion standpoint in that few wind turbines develop any useful energy below windspeeds of 11 ft/s (3.4 m/s).

Increase of Chord Thickness

At the outset of the wind turbine project, an optimum airfoil had not yet been determined. It was manifest that a thicker airfoil cross section would be advantageous for accommodating the expected bending stresses. Initially, therefore, an NACA 0024* cross section (as shown in Figure 3b) was selected for stress analysis considerations.

Thicker sections are preferable because, with this straight configuration, the blade stresses are predominantly bending; it is desirable, therefore, to have a large area moment of inertia with respect to the airfoil centerline axis (x-x in Figure 3). From the definition of the moment of inertia, $I_{xx} = \int y^2 dA$, it is noted that the value of this parameter rises rapidly with increased airfoil thickness. An NACA 0012 airfoil will have only about one-fourth the moment of inertia of an NACA 0024 airfoil if each has the same thin skin thickness as shown in Figure 3. Thus, the NACA 0012 airfoil actually used is half as thick as an NACA 0024 airfoil and, under the assumed conditions, can accommodate only one-fourth the bending load.

The NACA 0024 airfoil was assumed to be constructed similarly to that shown in Figure 3b, and analyses such as those presented herein were performed. The resultant bending stresses were still about 1 order of magnitude higher than can be permitted.

Troposkien Blade Stress Calculations

Assume that the same NACA 0012 blade cross section is used with a troposkien curved blade with both a diameter (D) and a height (H) of 15 feet. The troposkien shape allows only tensile stress along the blade, the least stress being at the midpoint and the highest near the hub at each end. Blackwell and Reis[2] developed the troposkien stress equation which, for $D/H \approx 1$, can be simplified to

$$\frac{T_{max}/A}{\rho\left(\frac{D}{2}\omega\right)^2} \approx 1 \tag{11}$$

where

T = blade tensile force (lbf)

ω = rotational velocity (70 rads/s)

A = solid cross-sectional area

Note that the numerator of Eq. (11) is a stress; i.e., $S_{max} = \frac{T_{max}}{A}$. Thus Eq. (11) can be rearranged as

*The maximum thickness is 24 percent of the chord.

$$S_{max} \approx \rho\left(\frac{D}{2}\,\omega\right)^2 = 29,000 \text{ psi } (2.00 \times 10^8 \text{ N/m}^2) \quad . \tag{12}$$

A safety factor based on a reasonable yield stress of 70,000 psi (4.8×10^8 N/m^2) for alloy steel would, therefore, be about 2.4.

Although this conservative design could permit operation at speeds higher than the 50 mph (80 km/hr) considered, it should be remembered that the tensile stresses increase with the square of the rotational speed (ω) and thus also with the square of the windspeed. For example, a 75-mph (120-km/hr) wind would produce blade stresses of over 65,000 psi (4.5×10^8 N/m^2), resulting in a safety factor of only 1.07.

Scale-Up Potential

From the work of Blackwell and Reis[1,2] it is noted that, for the rotationally induced stresses, the single-material parameter which affects the tensile stresses developed is the density of that material. Thus, the scale-up of a blade fabricated, as shown in Figure 3, from a single material will produce blade stresses of the same magnitude as the smaller scale version using that material. In general, the stresses produced for a blade of this design are a result only of blade velocity and material density and not of size.

For the squirrel-cage configuration, although the scaling effects are slightly more difficult to present in a closed-form expression, the results are similar. Also, since the stresses produced are bending stresses, they are heavily influenced by the airfoil cross section selected.

The rationale for the above conclusions is presented in Appendix A. The crux of this discussion is that the results presented for the 15-foot-diameter prototype wind turbine blades are the same as those that can be expected for larger scale designs. Regardless of the turbine size, the bending stresses produced in a turbine blade of squirrel-cage design are too large to permit this design to be considered as a practical alternative.

Conclusions

Curved and straight blade configurations of a 15-foot-diameter vertical-axis turbine have been analyzed to determine the expected stresses caused by rotation alone. For both designs a thin-shell cross section of airfoil shape, which appears desirable for optimum turbine performance and which would be reasonable to manufacture, was considered. The analysis shows that the high bending stresses inherent with the straight-blade design would preclude its selection as a practical candidate. The tensile stresses in the curved blade, however, permit operation in high winds while maintaining an acceptable safety factor.

Finally, it was shown that the results presented are applicable to systems of any size. Turbine systems will have nearly identical stress magnitudes for both large and small versions of the troposkien and squirrel-cage designs, respectively.

APPENDIX A

DEVELOPMENT OF SCALE-UP STRESS PREDICTIONS

Troposkien Tensile Stresses

Equation (12) is presented as

$$S_{max} \approx \rho \left(\frac{D}{2}\,\omega\right)^2$$

(with a restriction that $D/H \approx 1$).

The quantity in the parentheses is the blade speed, V_B, which has been assumed constant for this analysis. Thus, S varies only with ρ; i.e., no size factors influence the stress. It can also be shown that for <u>any</u> specified troposkien shape ($D/H \neq 1$) the same conclusion is valid.

Squirrel-Cage Bending Stresses

1. Except for the airfoil skin thickness not being increased, a linear scale-up of all the dimensions of the turbine and blade cross section is considered. Also, the blade velocity is a function of only the windspeed. For simplicity in presenting these results, assume that a thin-skin approximation of the airfoil cross section is valid. A characteristic length, L, will be applied to the various parameters considered in Eqs. (1) through (7) to ascertain the cumulative effect of a change in L:

(a) $I_{xx} \propto L^3$

The skin thickness remains constant.

(b) Blade weight $\propto L^2$

(c) Centrifugal acceleration $\propto \frac{1}{L}$

The blade speed is constant; therefore, ω is inversely proportional to L, acc $= R\omega^2$: $L \times \frac{1}{L^2} = \frac{1}{L}$.

(d) The total blade force $F_L \propto L$

The results of (b), above, multiplied by the results of (c), above

(e) The maximum moment $M \propto L^2$

$$M = \frac{F_L\,\ell}{8}: \; L \times L$$

(f) Bending stress $S \propto$ unity

$$S = \frac{Mc}{I}: \; \frac{L^2 \times L}{L^3} = \text{unity};$$

i.e., for the restricted example presented, the bending stresses produced are <u>not</u> a function of size.

2. The assumption that the metal skin thicknesses can remain constant is plausible only for sizes that are, perhaps, less than doubled. At the other extreme, it may be considered that all the assumptions presented still hold, except that now the airfoil skin thickness also increases linearly with turbine size increase.

The effect of L on the various parameters is considered sequentially as before:

(a) $I_{xx} \propto L^4$

(The thickness increase effect is now noticed.)

(b) Blade weight $\propto L^3$

(c) Centrifugal acceleration $\propto \frac{1}{L}$

(d) Total blade force $F_L \propto L^2$

(e) Maximum moment $M \propto L^3$

(f) Bending stress $S \propto$ unity

$$S = \frac{Mc}{I} : \frac{L^3 \times L}{L^4} = \text{unity}$$

Again it is observed that the bending stresses produced are <u>not</u> a function of size.

REFERENCES

1. B. F. Blackwell and G. E. Reis, Blade Shape for a Troposkien Type of Vertical-Axis Wind Turbine, Sandia Laboratories, SLA-74-0154, April 1974.
2. B. F. Blackwell and G. E. Reis, Some Geometrical Aspects of the Troposkien as Applied to Vertical-Axis Wind Turbines, Sandia Laboratories, SAND74-0177, November 1974.
3. B. F. Blackwell, The Vertical Axis Wind Turbine "How It Works," Sandia Laboratories, SLA-74-0160, April 1974.

DISTRIBUTION:

J. Templin
Low Speed Aerodynamics Section
NRC-National Aeronautical Establishment
Ottawa 7, Ontario, Canada K1AOR6

A. Robb
Memorial University of Newfoundland
Faculty of Engineering & Applied Sciences
St. John's, Newfoundland
Canada A1C 5S7

H. Sevier
Rocket and Space Division
Bristol Aerospace Ltd.
P. O. Box 874
Winnipeg, Manitoba
R3C 2S4 Canada

B. D. Henshall
Acting Executive Officer
The University of Auckland
Private Bag
Auckland, New Zealand

G. Herrera
Jet Propulsion Lab
4800 Oak Grove Drive
Pasadena, CA 91103

NASA Langley Research Center
Hampton, VA 23365
Attn: R. Muraca, MS 317

NASA Lewis Research Center
21000 Brookpark Road
Cleveland, OH 44135
Attn: J. Savino, MS 500-201

ERDA (2)
1800 G Street NW
Washington, D. C. 20550
Attn: L. Divone
J. Rannels

B. Vance
Science Applications
1200 Prospect Street
La Jolla, CA 92073

A. N. L. Chiu
Wind Engineering Research Digest
Spalding Hall 357
University of Hawaii
Honolulu, HI 96822

R. N. Meroney
Colorado State University
Dept. of Civil Engineering
Fort Collins, CO 80521

Chumin Fu
Illinois Institute of Technology
Department of Physics
Chicago, IL 60616

New Mexico State University (3)
P. O. Box 3450
Las Cruces, NM 88003
Attn: H. A. Daw
M. M. Sluyter
R. San Martin

Oklahoma State University
Stillwater, OK 74074
Attn: D. K. McLaughlin, ME Department

Oregon State University
Corvallis, OR 97331
Attn: R. Wilson, ME Department

Texas Tech University (2)
Lubbock, TX 79409
Attn: K. C. Mehta, CE Department
J. Strickland, ME Department

R. G. Watts
Tulane University
Department of Mechanical Engineering
New Orleans, LA 70118

University of New Mexico (2)
Albuquerque, NM 87106
Attn: K. T. Feldman, Energy Research Center
V. Skoglund, ME Department

Nevada Operations Office, ERDA (2)
P. O. Box 14100
Las Vegas, NV 89114
Attn: R. Ray, Operations
H. Mueller, ARL

Los Alamos Scientific Laboratory (6)
P. O. Box 1663
Los Alamos, NM 87544
Attn: R. R. Brownless, J-DO
J. R. Bartlit, Q-26
J. D. Balcomb, Q-DO-T
R. G. Wagner, P-5
J. Nachamkin, E-DOR
S. Depp, E-DO

ERDA/ALO (3)
Kirtland AFB East, NM 87115
Attn: D. W. King
J. R. Cotton

R. Camarero
Faculty of Applied Science
University of Sherbrooke
Sherbrooke, Quebec
Canada J1K 2R1

American Wind Energy Association
21243 Grand River
Detroit, MH 48219

DISTRIBUTION CONT:

E. E. Anderson
Department of Mechanical Engineering
South Dakota School of Mines and Technology
Rapid City, SD 57701

M. Snyder
Aero Engineering Department
Wichita State University
Wichita, KS 67208

R. A. Parmelee
Department of Civil Engineering
Northwestern University
Evanston, IL 60201

Ralph Beckman
Research and Design Institute
P. O. Box 307
Providence, RI 02901

Binx Selby
5595 E. Arapaho
Boulder, CO 80302

J. Park
Helion
Box 4301
Sylmar, CA 91342

W. F. Foshag
Aerophysics Co.
3500 Connecticut Ave., NW
Washington, DC 20008

W. L. Harris
Aero/Astro Department
MIT
Cambridge, MA 02139

K. Bergey
Aero Engineering Department
U. of Oklahoma
Norman, OK

J. Fischer
F. L. Smidth & Co A/S
Vigerslevallé 77
2500 Valby
Denmark

H. M. Busey
DMA, Safety and Facilities A-364
ERDA Headquarters
Washington, DC 20545

O. Krauss
Div. of Engineering Research
Michigan State University
East Lansing, MI 48823

1544 L. I. Weingarten
4700 D. B. Shuster, Attn: V. L. Dugan, 4734
5000 A. Narath
5600 A. Y. Pope, Attn: R. C. Maydew, 5620
5623 E. C. Rightley, Attn: L. V. Feltz, 5623
5628 S. McAlees, Jr.
5628 B. F. Blackwell (100)
5640 K. J. Touryan
5700 J. H. Scott, Attn: G. E. Brandvold, 5710
5712 R. H. Braasch (3)
Attn: E. G. Kadlec
J. A. Leonard
A. F. Veneruso
5717 R. P. Stromberg (2)
Attn: D. E. Randall
B. W. Marshall
5844 B. L. Butler
8000 T. B. Cook, Jr.
8100 L. Gutierrez, Attn: A. N. Blackwell, 8110
8266 E. A. Aas (2)
9480 J. E. Stiegler (2)
Attn: W. V. Hereford, 9483
T. C. Looney, 9483
3141 L. S. Ostrander (5)
3151 W. F. Carstens (3)
For ERDA/TIC (Unlimited Release)